# AIAA 2001–0016

## LATERAL TRACK CONTROL LAW FOR AEROSONDE UAV

Marius Niculescu
*University of Washington, Seattle, WA 98195*

**39th AIAA Aerospace Sciences Meeting and Exhibit**
**8–11 January 2001 / Reno, NV**

# LATERAL TRACK CONTROL LAW FOR AEROSONDE UAV

Marius Niculescu*
*University of Washington, Seattle, WA 98195*

**Aerosonde is a small autonomous aircraft (UAV) designed for meteorological sampling along a specified flight plan. This aircraft is currently being used by the Flight Systems Laboratory at the University of Washington as a test-bed for the development of a rapid control-law prototyping platform based on Matlab/Simulink/Real-Time Workshop environment. To accurately track a set of pre-planned flight segments, an automatic lateral-track control law was developed and implemented in Aerosonde I. However, the early design of the lateral track control-law was found to have unsatisfactory tracking performance in the presence of large cross-track distance errors, and/or when the aircraft is pointing away from the desired flight plan segment. The track performance was subsequently improved by the use of complex decision logics imbedded in the custom autopilot software, thereby making the controller unsuitable for future UAV projects. A new nonlinear lateral track control law has been proposed and results are presented in this paper. It will be shown that with the new design which does not require complex switching decision logics, the aircraft is able to stably track a flight plan segment starting from any initial conditions. In high wind situations, lateral tracking and stability are achieved with a modified control law that directly utilizes the wind information. Performance of the overall lateral track control law has been verified in nonlinear flight simulations.**

## Nomenclature

| | |
|---|---|
| **UAV** | Unmanned Air Vehicle |
| **GPS** | Global Positioning System |
| **MEX** | Matlab Executable |
| **DOF** | Degrees of Freedom |
| $X_{track}$ | Along-track distance (m) |
| $Y_{track}$ | Cross-track distance (m) |
| $\dot{X}_{track} = dX_{track}/dt$ | Along-track velocity (m/s) |
| $\dot{Y}_{track} = dY_{track}/dt$ | Cross-track velocity (m/s) |
| $U$ | Airspeed (m/s) |
| $W$ | Wind speed (m/s) |
| $r_{CMD}$ | Yaw-rate command (rad/s) |
| $\Psi$ | Aircraft heading (rad) |
| $\Psi_w$ | Wind direction (rad) |
| $\Psi_{12}$ | Track line heading (rad) |
| $\Delta$ | Discrete-time step (s) |

## Introduction

### Vehicle Description

Aerosonde is a small autonomous airplane designed for long-range weather data acquisition. It was developed especially for reconnaissance over oceanic and remote areas, and in harsh conditions. Its low-cost design and operational flexibility will promote its usage for a wide range of remote-sensing applications. Aerosonde development started in 1992 when the concept was first proposed in a research paper by McGeer.[1] The main subcontracting organizations for the early development work were the Insitu Group in the USA and the Australian Bureau of Meteorology. The airplane Aerosonde Phase I project was completed and the vehicle is currently marketed and operated by Aerosonde Robotic Aircraft Ltd of Australia. Table 1 lists the characteristics of the Phase I Operational Aerosonde. In August 1998, Aerosonde "Laima", one of ten aircraft delivered to University of Washington under a contract from the US Office of Naval Research, became the first robotic aircraft to cross the North Atlantic. Laima took off from Bell Island in Newfoundland and safely landed on Benbecula Island in the Outer Hebrides after a 26 hr 45 min autonomous flight.

**Table 1 Parameters of Phase I Operational Aerosonde**

| | | |
|---|---|---|
| Vehicle characteristics | Wing span | 2.9 m |
| | Gross weight | 13-14 kg |
| | Payload | 1 kg |
| Performance | Cruise speed | 20-30 m/s |
| | Max. speed | 30-40 m/s |
| | Max. altitude | 5000 m |
| | Range | 2500-3000 km |
| | Endurance | 30-35 hr |
| | Engine | 26 cc petrol |
| | Take-off | Car roof rack |
| | Landing | On belly |
| | Operation | Autonomous |
| | Navigation | GPS |
| | Communication | UHF Radio, Satellite (under development) |
| Weather data acquisition | Altitude | |
| | Wind | |
| | Pressure | |
| | Temperature | |
| | Moisture | |

*Graduate Student, Department of Aeronautics and Astronautics. Student member AIAA

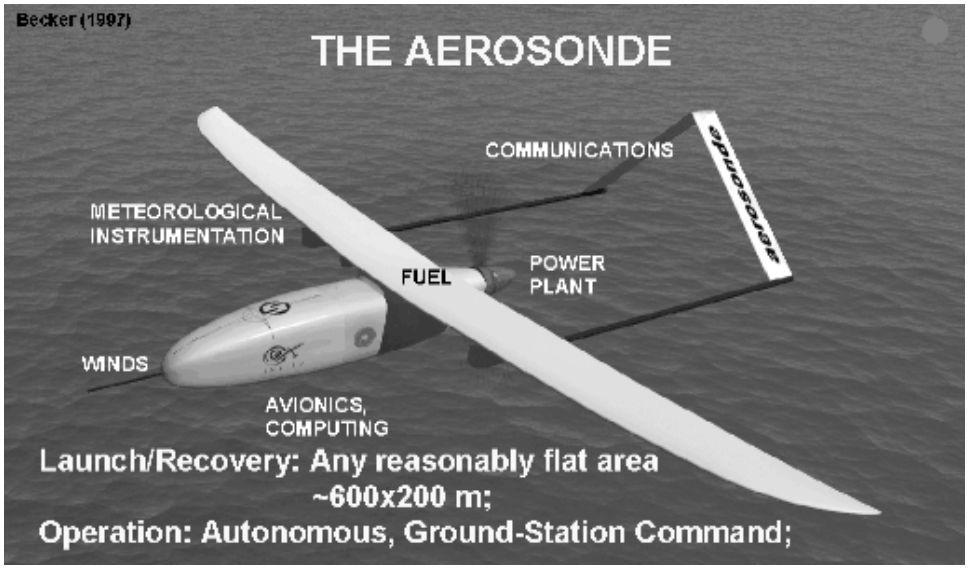


**Fig. 1 The Aerosonde** ***(Image by Jon Becker, Aerosonde Robotic Aircraft)***

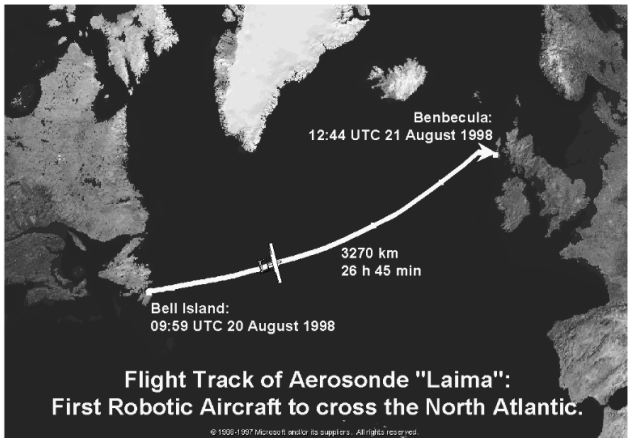


**Fig. 2 Trans-Atlantic Flight**

**Current Development**

Presently, the Flight Systems Laboratory focuses its research on the development of a rapid prototyping platform for UAV control systems using Phase I Operational Aerosonde as a test-bed. The software implementation is based on Matlab/Simulink user-friendly environment* . Flight control laws will be implemented and tested in Simulink. Decision logic and switching between different autopilot functions can be coded graphically in Stateflow diagrams. Once the desired performance of the complete flight control systems has been achieved and verified in closed-loop nonlinear simulations, the entire autopilot block diagrams can be automatically converted into C code using Real-Time Workshop. The resulting C code is then compiled, linked and uploaded to the flight control computer (presently implemented in a Tattle 8 microprocessor). The real-time controller can then be tested in hardware-in-the-loop simulations. A nonlinear 6-DOF aircraft model (also in Matlab) emulates sensor output signals to the autopilot computer and receives back as inputs real-time control signals from the autopilot. Different forms of graphical outputs can be generated which include real-time plots of various flight parameters, animated map display, virtual cockpit, and external view of the airplane in Microsoft Flight Simulator, or other 3-D graphical interfaces.

**Description of Existing Lateral Track Control**

The sensors available for the lateral track control consist of a yaw rate gyro and a GPS sensor which provides the position and ground speed of the aircraft. There are neither compass nor roll-rate gyro onboard. The GPS signal is used to compute the track distance and velocity to the current flight plan segment expressed in terms of cross-track $(Y_{track}, \dot{Y}_{track})$ and along-track $(X_{track}, \dot{X}_{track})$ components. The primary design objective of the lateral controller is to intercept and track a specified flight plan segment while ensuring that the vehicle yaw rate does not exceed 0.2 rad/s in amplitude. To achieve this design objective, a lateral control law was implemented on the Phase I Aerosonde's autopilot consisting of an inner-loop control, which takes a yaw-rate command $r_{CMD}$ as input and computes the necessary aileron and rudder commands. The desired $r_{CMD}$ is determined from an outer-loop lateral-track control based on the cross-track variables $Y_{track}$ and $\dot{Y}_{track}$ (Figure 3). As mentioned in the Aerosonde Flight Control Specifications,[2] the airplane was not able to follow to the desired track when there are excessive errors in either cross-track distance, velocity or heading. To address this problem, complex decision logics were introduced into the autopilot code, and for each situation appropriate maneuvers (such as performing hard turns or flying straight) are initiated so that the airplane is positioned along a much favorable path prior to activating the lateral track control law. This customized and complicated switching schemes make the lateral tracker difficult to generalize in a rapid prototyping platform. Ideally, we would like to have standardized control function blocks which can be easily implemented

*Matlab, Simulink, Stateflow are trademarks of MATHWORKS, Inc.

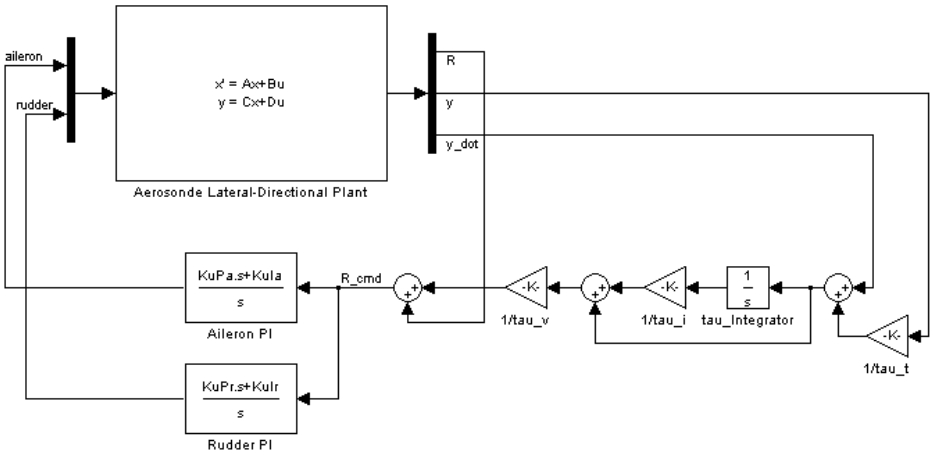


**Fig. 3 Existing Lateral Control Block Diagram**

in a generic UAV flight control systems where changes in the design would involve only the tuning of a set of well-defined design gain parameters. Moreover, the existing control design exhibited Dutch-roll instability which was first noticed during flight tests, and later duplicated on the hardware-in-the-loop simulator. Figure 4 shows a screen capture from the Aerosonde ground station where we can clearly see the Dutch-roll instability which led to large oscillations in cross-track distance with an amplitude of approximately 10 m during an automatic landing. In

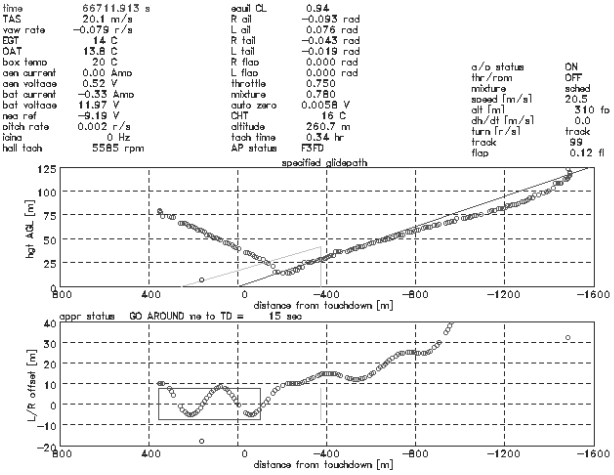


**Fig. 4 Excessive Lateral Oscillations during an Automatic Landing *(Aerosonde Ground-Station Screen)***

the summer of 1999, extensive redesign of the inner-loop lateral control law was performed using a nonlinear optimization design tool SANDY.[3] As many as 63 linearized airplane models corresponding to various airplane configurations and flight conditions were generated and used in the design optimization of the lateral tracker proportional and integral gains. It was noticed that in order to achieve a robust design with the given controller structure over the entire range of flight conditions, trade-offs must be made in stability and robustness performance. For example, upper bounds of the constrains on the real part of the closed-loop eigenvalues must be set to $-0.001$, and even to 0 for neutral stability in some design conditions. Moreover, lower bounds on the damping constrains must also be reduced from 0.4 to 0.2 in order to achieve a feasible solution in the design optimization.

## Vehicle Kinematic Model

**Continuous-Time Dynamic Model**

A nonlinear 6-DOF model of Aerosonde in Matlab/Simulink environment was not available at the time we started the design work on a new lateral track control law. Instead a vehicle kinematic model was created that would capture all the key parameters in the lateral track control design including the wind effects. The vehicle kinematic model is much simpler than a full nonlinear simulation model and it enables us to quickly evaluate our lateral track control law in closed-loop simulation. Let's consider an Aerosonde in level flight at an arbitrary position relative to the track line between way points $W_{p1}$ and $W_{p2}$, and flying on an arbitrary heading $\Psi$. We adopt the following notations: $\Psi = \angle(\vec{U}, Y_{North})$, $\Psi_w = \angle(\vec{W}, Y_{North})$ and $\Psi_{12} = \angle(< W_{p1}, W_{p2} >, Y_{North})$. Given the airplane velocity and position in the <North,East> reference frame, we are interested to obtain the position and velocity components in the $< X_{track}, Y_{track} >$ reference frame. The transformation will be a rotation of an angle $(\Psi_{12} - \pi/2)$ and the associated rotation matrix is given by

$$T_\Psi = \begin{bmatrix} \cos(\Psi_{12} - \pi/2) & -\sin(\Psi_{12} - \pi/2) \\ \sin(\Psi_{12} - \pi/2) & \cos(\Psi_{12} - \pi/2) \end{bmatrix} \quad (1)$$

Applying the above rotation to the airspeed and windspeed vectors, we obtain

$$\vec{U}_{track} = T_\Psi \vec{U} \quad (2)$$

and

$$\vec{W}_{track} = T_\Psi \vec{W} \quad (3)$$

Along-track and cross-track velocities can be written as

$$\begin{cases} \dot{X}_{track} &= U_{track_x} + W_{track_x} \\ \dot{Y}_{track} &= U_{track_y} + W_{track_y} \end{cases} \quad (4)$$

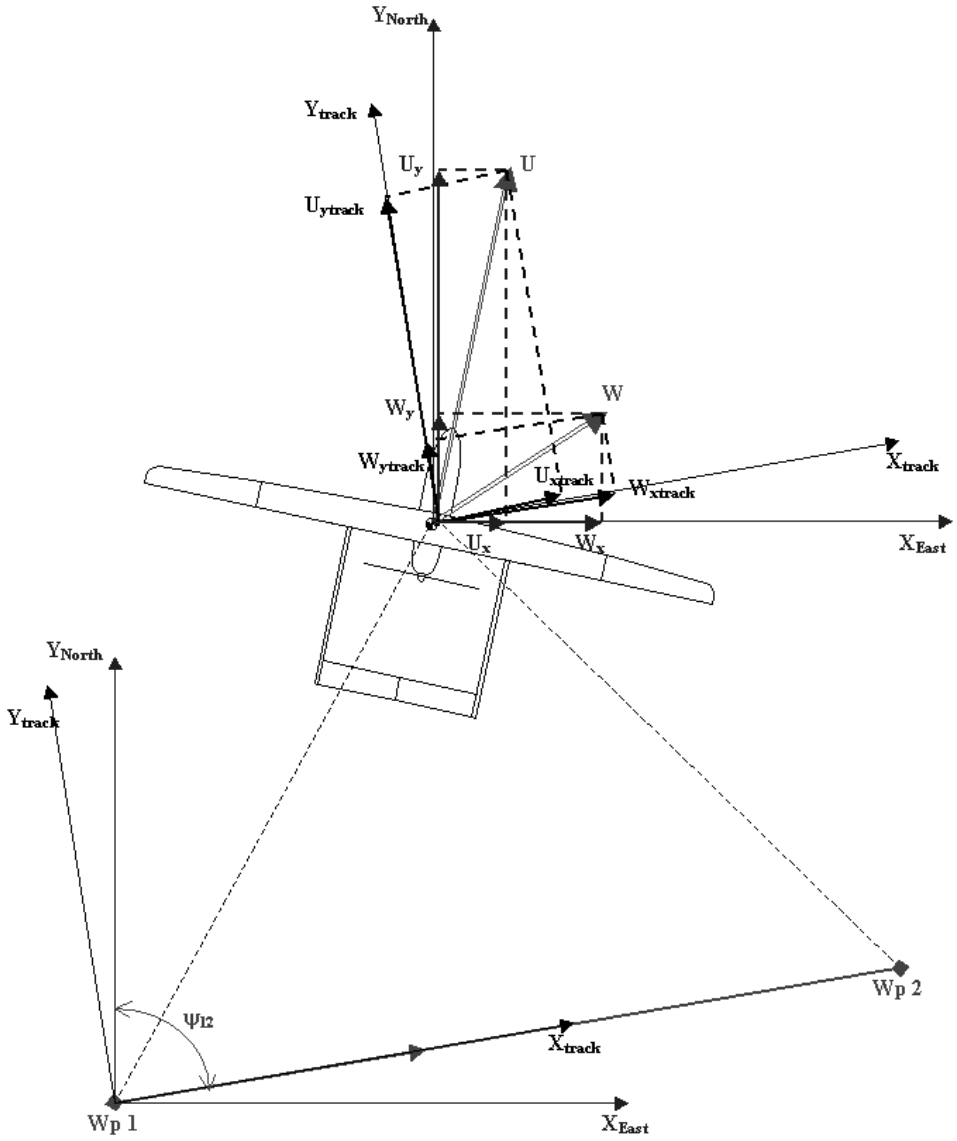


**Fig. 5 Vehicle Kinematic Analysis**

Therefore, the continuous-time vehicle kinematic model is described by the following set of nonlinear differential equations:

$$\begin{cases} \dot{X}_{track}(t) &= U\cos(\Psi(t)-\Psi_{12}) + W\cos(\Psi_w-\Psi_{12}) \\ \dot{Y}_{track}(t) &= -U\sin(\Psi(t)-\Psi_{12}) - W\sin(\Psi_w-\Psi_{12}) \\ \dot{\Psi}(t) &= r_{CMD}(t) \end{cases} \tag{5}$$

To further simplify the problem, the following assumptions have been made:

- $U$ =constant with the airspeed-hold loop enabled,
- $W$ =constant, $\Psi_w$ =constant (no changes in wind conditions), and
- $\Psi_{12}$ =constant (no changes in flight plan).

**Discretization of Vehicle Kinematic Model**

A first-order integration scheme is used to discretize the continuous-time kinematic model. The discretization should yield acceptable results when the time step $\Delta$ is kept small. The discretized dynamic model is as follows:

- State vector:

$$\vec{x}(t) = \begin{bmatrix} X_{track}(t) \\ Y_{track}(t) \\ \Psi(t) \end{bmatrix} \tag{6}$$

- Control variable:

$$u(t) = r_{CMD}(t) \tag{7}$$

- Discretized system dynamics:

$$\vec{x}(i+1) = \vec{f}(\vec{x}(i), u(i), \Delta) =$$

$$\begin{bmatrix} X_{track}(i) + \Delta\cdot[U\cos(\Psi(i)-\Psi_{12}) + W\cos(\Psi_w-\Psi_{12})] \\ Y_{track}(i) + \Delta\cdot[-U\sin(\Psi(i)-\Psi_{12}) - W\sin(\Psi_w-\Psi_{12})] \\ \Psi(i) + \Delta\cdot r_{CMD}(i) \end{bmatrix} \tag{8}$$

- Initial conditions:

$$\vec{x}(0) = \begin{bmatrix} X_{track_o} \\ Y_{track_o} \\ \Psi_o \end{bmatrix} \tag{9}$$

## Lateral Track Control Strategy

The design problem is to develop a lateral track control that guides the Aerosonde to the destination way point $W_{p2}$ along a track line defined by the way points $W_{p1}$ and $W_{p2}$ as depicted in Figure 6 by means of a yaw-rate command. Knowing the current track position $(X_{track}, Y_{track})$ of the vehicle from the destination way point $W_{p2}$, the control strategy is to point the vehicle ground speed vector $\vec{V}$ in the direction of the track intercepting the track line at point C. The intercept point C is determined by a design parameter $k$ where the distance on the track line from the intercept point $C$ to the way point $W_{p2}$ is at any instant of time equal to $(1-k)X_{track}$. From the geometry of the similar triangles $OAB$ and $OCD$, a new control strategy is proposed based on establishing the vehicle position and velocity according the following relationship,

$$\frac{\dot{X}_{track}}{kX_{track}} = \frac{\dot{Y}_{track}}{Y_{track}} \tag{10}$$

To achieve this objective, the error $E$ given by

$$E = kX_{track}\dot{Y}_{track} - Y_{track}\dot{X}_{track} = 0 \tag{11}$$

is to be driven to zero using a proportional feedback control law that expresses the yaw-rate command as

$$r_{CMD} = K_R E = K_R \left(kX_{track}\dot{Y}_{track} - Y_{track}\dot{X}_{track}\right) \tag{12}$$

where the proportional gain $K_R$ is determined iteratively thru simulation until good tracking is achieved with virtually no overshoot. A value of $K_R = -0.0025$ was found to be satisfactory in our lateral track control law. For safety purpose, we need to impose a limit of $R_{max} = \pm 0.2$ rad/s on the yaw-rate command $r_{CMD}$. The actual yaw-rate command to the inner-loop of the lateral control law is implemented as output of a saturation function. Namely,

$$r_{CMD} = sat\left(K_R\left[kX_{track}\dot{Y}_{track} - Y_{track}\dot{X}_{track}\right]\right) \tag{13}$$

where the saturation function $sat(-)$ is defined as follows,

$$sat(u) = \begin{cases} -R_{max} & , \quad u & < -R_{max} \\ u & , \quad |u| & < R_{max} \\ R_{max} & , \quad u & > R_{max} \end{cases} \tag{14}$$

A Simulink block diagram that realizes the control scheme described in equation (13) is shown in Figure 7.

## Simulation Results

Evaluation of the proposed lateral track control described in Section  is performed using two types of models:

1. A discretized vehicle kinematic model as presented in Section , and
2. A full 6-dof nonlinear simulation model of the Aerosonde with its complete set of longitudinal and lateral autopilots.

**Simulation using Discretized Vehicle Kinematic Model**

Advantage of this simulation model is its simplicity and thereby providing a rapid turnaround in the analysis of the closed-loop tracking performance. Here, we basically assume that the vehicle yaw rate matches instantaneously the commanded yaw rate $R_{CMD}$ ignoring the vehicle inertia and its dynamics. Figure 8 shows a map of the flight plan segment between the way points $W_{p1}$ and $W_{p2}$ (in red). The starting position and heading of the vehicle is shown with the Aerosonde profile. The resulting flight path achieved under the new lateral track control design as the airplane moves toward the way point $W_{p2}$ is shown also shown. In this simulation, the wind speed $W$ is assumed zero and the Aerosonde airspeed is held constant to 20 m/s. As mentioned previously, the lateral track controller uses a proportional gain of $K_R = -0.0025$ and a design parameter $k$ of 0.2. The $x$ and $y$-axes of the map are oriented East and North respectively, and the dimensions are given in meters. We can see that the airplane successfully reaches the desired way point $W_{p2}$ starting from any arbitrary location and heading. In Figure 9, the simulation was performed with the airplane states set to the same initial conditions in track positions and heading while we vary the design parameter $k$ in the control law. It can be seen that the factor $k$ can be conveniently used to produce a different curvature for the Aerosonde track trajectory. When $k = 0$, the vehicle approaches the way point $W_{p2}$ along a line perpendicular to the track, while for $k \geq 1$ the airplane will fly straight to the way point $W_{p2}$ without intercepting the track line segment between the way points $W_{p1}$ and $W_{p2}$. It is found from extensive simulation that the airplane has no difficulty to arrive at the destination way point $W_{p2}$ even in the presence of wind, as long as the wind speed $W$ is less than the airspeed $U$. In Figure 10, the Aerosonde is assumed to maintain a constant airspeed of $U = 20$ m/s and the wind has a constant heading and a magnitude of $W = 10$ m/s. Snapshots of aircraft positions and orientations are taken periodically throughout the maneuver showing the different effects wind has on the airplane headings. Cases where the wind speed exceeds the vehicle airspeed will be treated in Section .

**Simulation using Nonlinear Aerosonde Model in Matlab/Simulink**

A nonlinear 6-dof airplane model was later developed using the aerodynamics and propulsion models extracted from the existing Aerosonde simulator. The original C-codes of these models are first converted to Matlab MEX-files, and calls to these functions are carried out in a Simulink S-function. The S-function for the vehicle nonlinear flight dynamics was written to compute the time derivatives of all state variables, which are then integrated using either one of Simulink's built-in integration schemes. The closed-loop model shown in Figure 11 depicts a complete autopilot diagram for the longitudinal and lateral control systems which include an altitude and airspeed-hold autopilot, a pitch damper, a gain schedule and a flight plan-

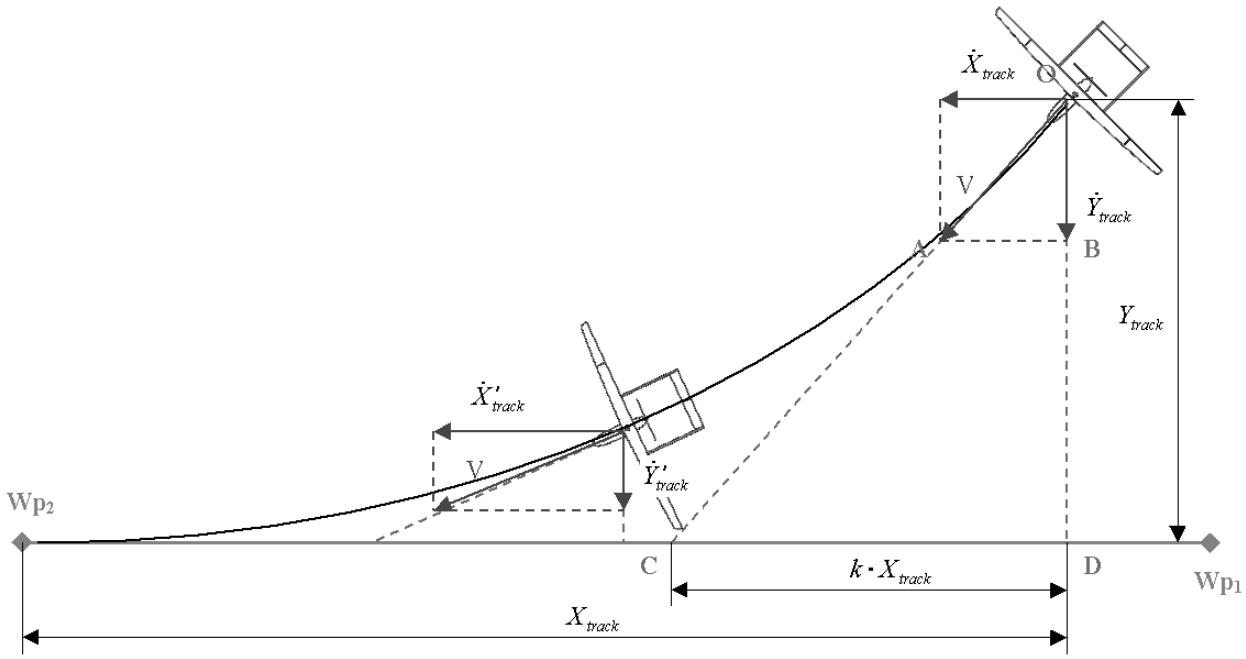


**Fig. 6 Lateral Track Control Strategy**

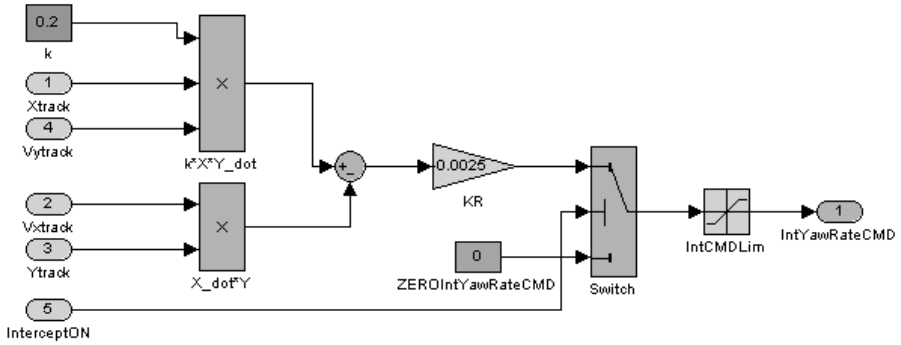


**Fig. 7 Lateral Track Control Diagram**

ner created using the Stateflow toolbox. The function of the flight planner is to provide the lateral track controller with the position and orientation of the current flight plan segment. Figure 12 displays a map of the Aerosonde trajectory starting from an initial position inside a box-shaped flight plan. The airplane trajectory is displayed over a time span of $1,000$ seconds. Figure 13 shows the time responses of vehicle roll rate and roll angle during the track maneuver. The simulation points out the presence of large oscillations in the vehicle roll responses. This phenomena occurs due to the coupling between the vehicle lateral dynamics and the lateral track control. The dynamic coupling is found to be significant between the outer-loop lateral track control and the inner-loop yaw control. Note that the simple kinematic model used in the lateral track control design did not include the yaw control loop and the vehicle lateral dynamics and therefore cannot be used to evaluate the dynamic coupling. In realistic situations, the airplane has measurable delay in responding to a yaw rate command. The slow dynamic responses of the vehicle cause the lateral track controller output to limit-cycle between the saturation values of $\pm 0.2$ rad/s. This limit-cycle problem was resolved by adding a roll-off filter to the lateral track control loop. Finally, we combine together the filter and the existing proportional gain to obtain the modified control design whose block diagram is shown in Figure 14. With this modification, the roll responses are much improved with adequate settling times and no limit cycles. We can see in Figure 15 that for a simulation on the same box-shaped flight plan, the roll rate responses are excited only when the aircraft is turning toward the next waypoint, and the subsequent oscillations are sufficiently damped after the turn maneuver.

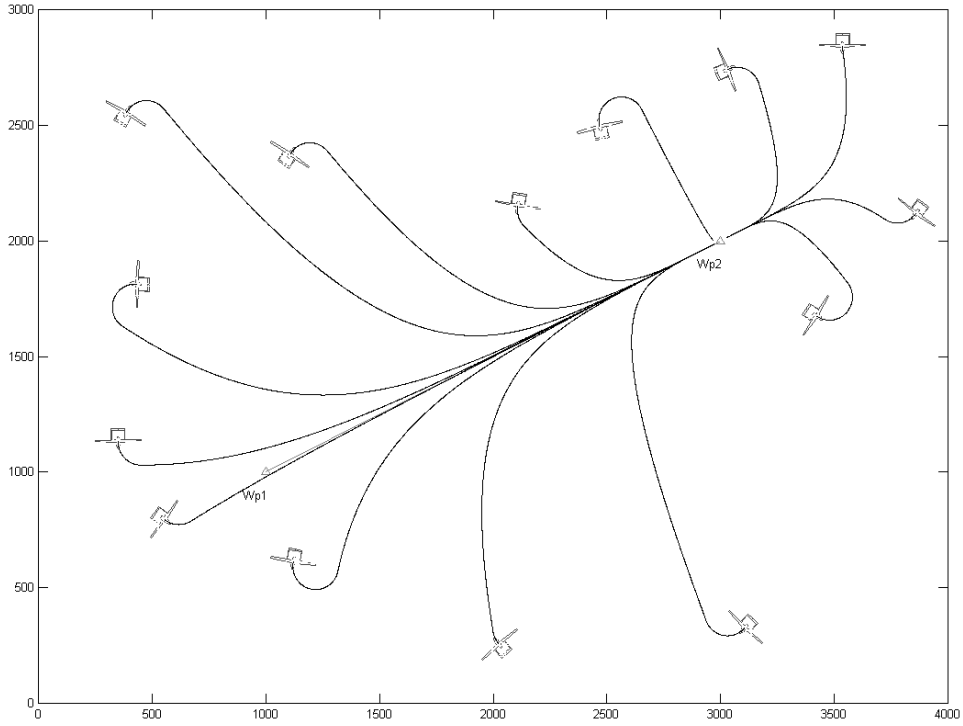


**Fig. 8 Simulation of Lateral Track Control in Zero Wind**

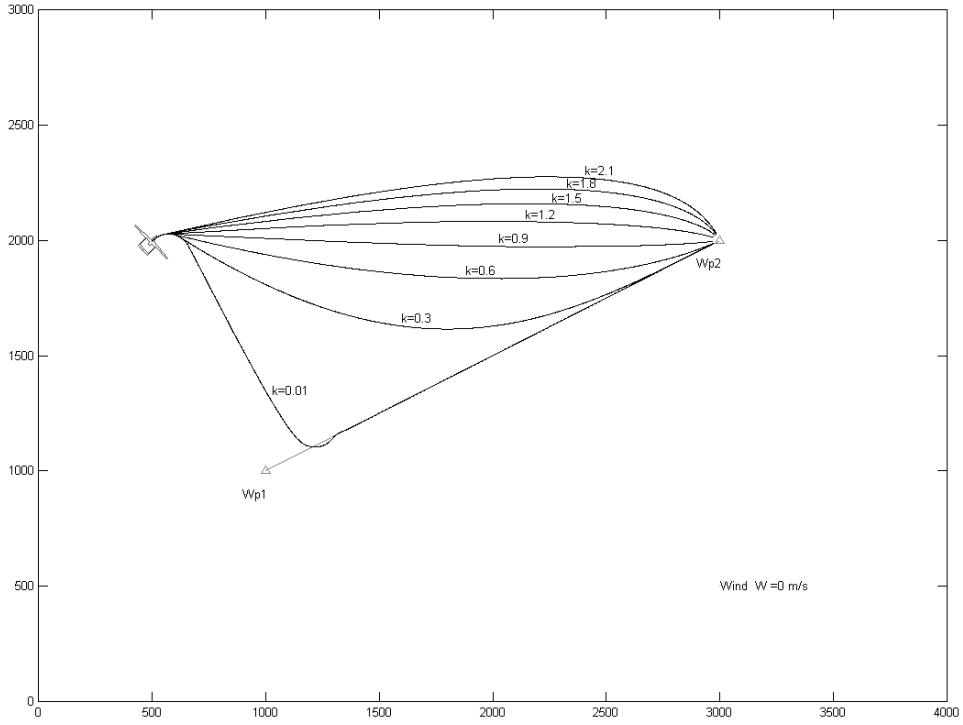


**Fig. 9 Influence of the Design Parameter *k* on Lateral Track Control**

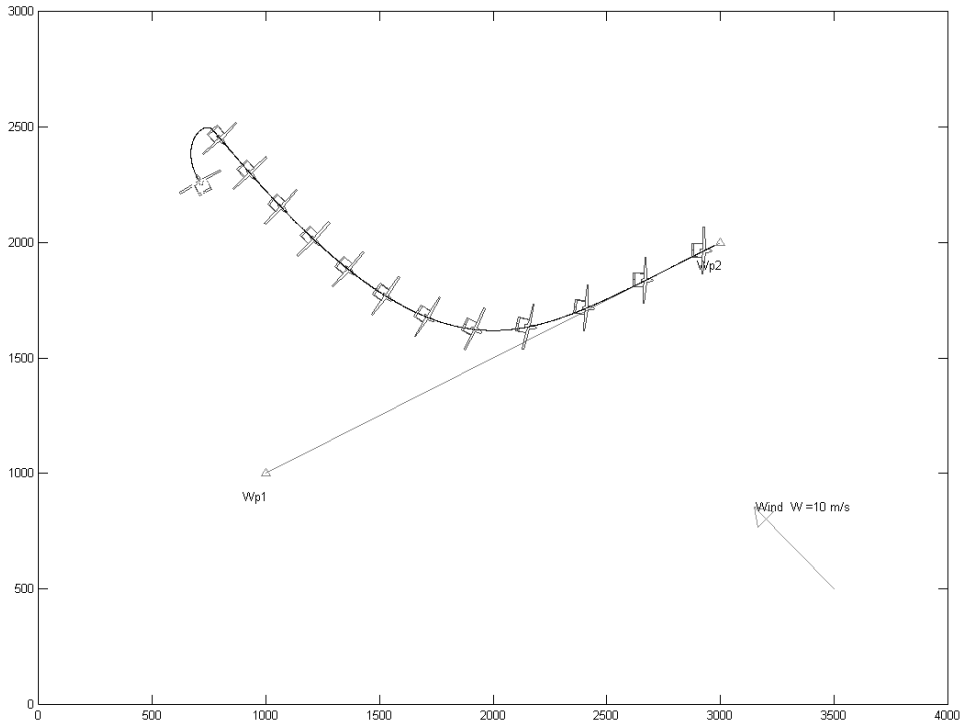


**Fig. 10 Influence of Wind to Lateral Track Control Performance**

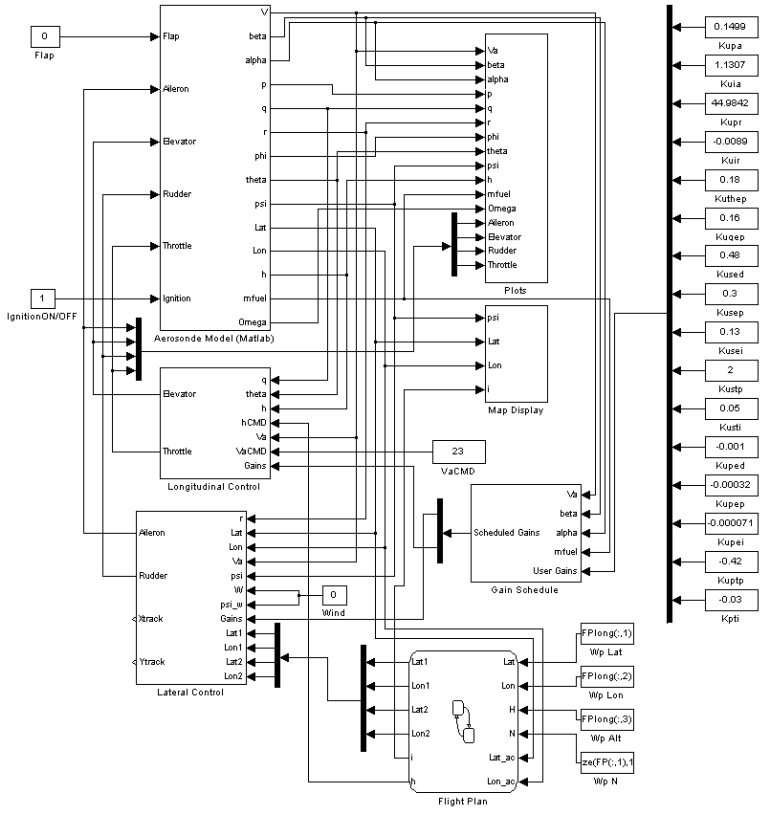


**Fig. 11 Aerosonde Simulation in Matlab/Simulink**

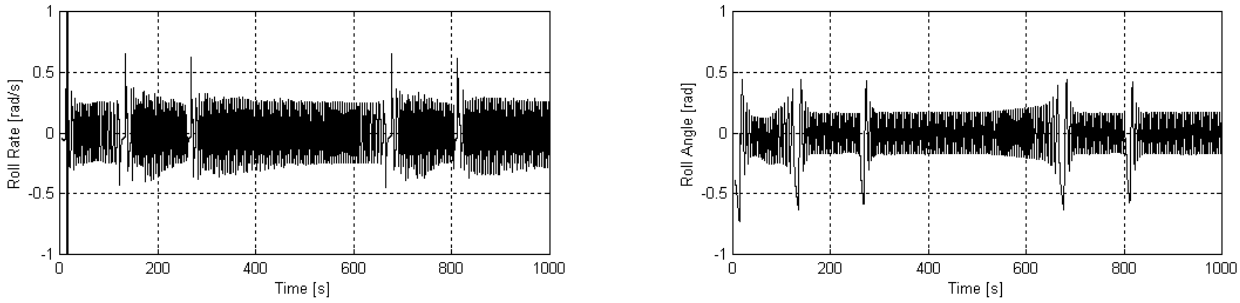


**Fig. 13 Roll Rate and Angle Responses during the Track Maneuver in Matlab/Simulink Simulation**

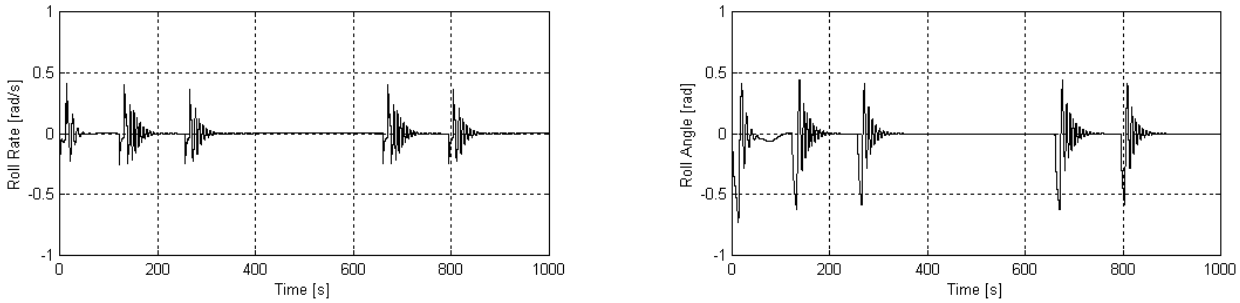


**Fig. 15 Roll Rate and Roll Angle Responses with the Modified Lateral Track Control Law**

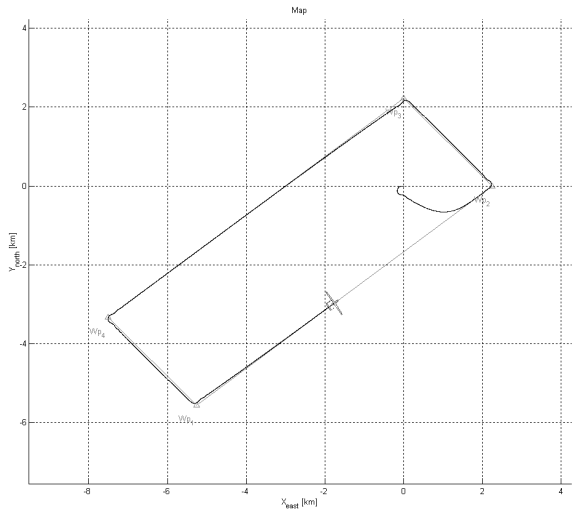


**Fig. 12 Map of the Flight Plan**

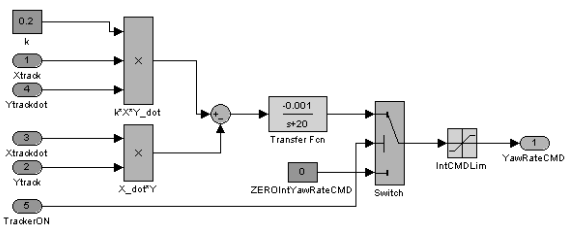


**Fig. 14 Modified Lateral Track Control Law with Roll-Off Filter**

## High-Wind Cases

In this section we address the control design problems associated with the high-wind cases. Since Aerosonde is a weather reconnaissance UAV, it is not uncommon for the vehicle to encounter strong winds during the mission. In some cases, the wind speed may far exceed the airplane's maximum operating speed. Thus, most likely the Aerosonde will no longer be capable to reach the desired way points or converge toward the flight plan segments. One of the design requirements in the lateral track control law is to identify whether the airplane can fulfill the desired flight plan segment and, if not, how to establish an alternate and more feasible design goal in transition. One option we examine is for example to initiate a heading-hold control into the wind while waiting for the wind intensity to subside. In the next two sections, we illustrate the design problems associated with high-wind conditions and present a new modified control-law that provides a stable maneuver of the vehicle into the wind.

#### Simulation Results in High-Wind Cases

Let's consider the situation where the wind is of magnitude 25 m/s which is greater than the vehicle airspeed of 20 m/s and in a direction normal to the flight plan segment to be tracked. Only the simple kinematic model of the airplane is used in the following simulation. Snapshots of the airplane position and orientation are taken at regular time intervals (Figure 16). Clearly, as expected the airplane is blown away from the track by the wind while maintaining stable trajectories as it points itself into the wind and flies backward. However, if the wind direction is along the track toward the way point $W_{p2}$, the Aerosonde would now travel with the wind coming from the rear. In this case, the

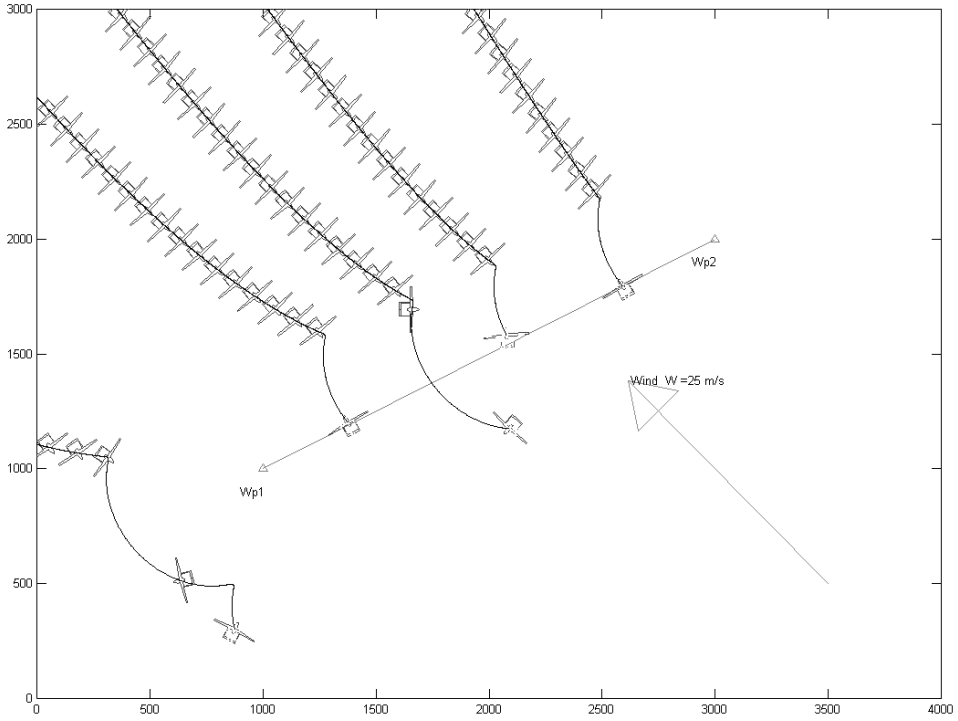


**Fig. 16 Track Performance in Cross Wind**

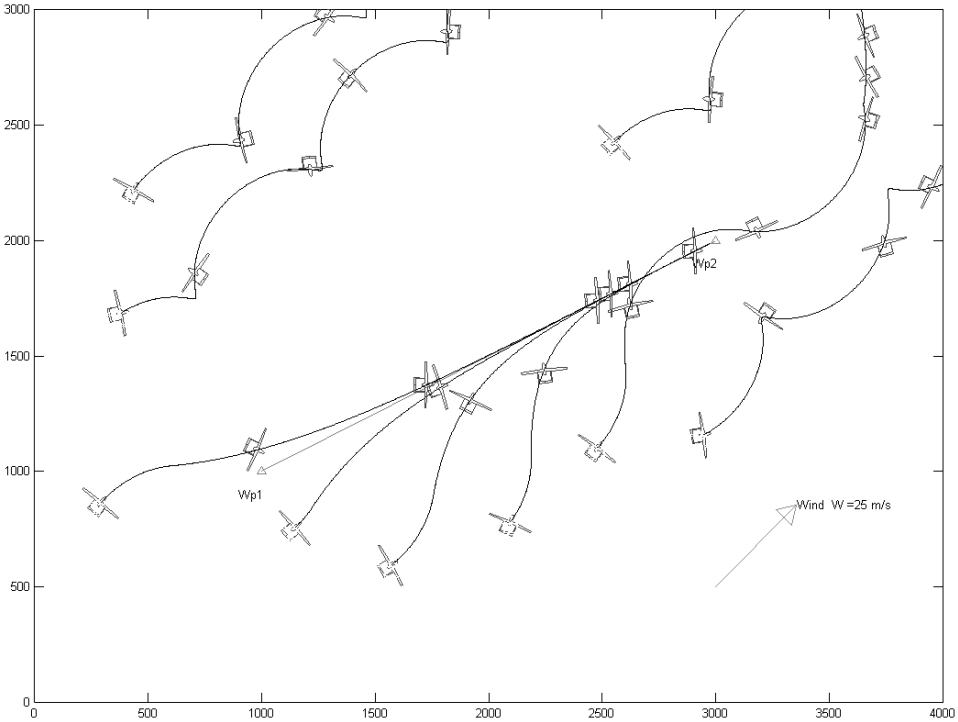


**Fig. 17 Track Performance in Tail Wind**

ground speed of the airplane would be so high that the yaw rate command is saturated inside the lateral track control. In this case, the airplane may or may not converge to the desired way point $W_{p2}$ depending on how far it is from the track line initially (Figure 17). When it fails to converge to the track, the lateral track controller would send a yaw-rate command saturated at the maximum amplitude of 0.2 rad/s to the inner loop which then places the airplane into a persistent unrecoverable turn. Figure 17 shows the simulation for the case of a 25 m/s wind blowing from the East and parallel to the track line.

**Modified Control Law for High-Wind Cases**

A solution to the case of high-wind instability mentioned in the previous section is to adopt a different control law when this condition is detected. The control law proposed is

$$r_{CMD} = K'_R(\Psi - \pi - \Psi_w) + K''_R Y_{track} \qquad (15)$$

The control law is making use of the estimated heading $\Psi$ and its design contains two terms. The first term is used to drive the airplane heading into the wind and to maintain track stability, while the second term is used to reduce the airplane cross-track distance. A simulation of the vehicle responses using the new control law for the case of an along-track wind of 25 m/s is shown in Figure 18. Note that the trajectories change to a darker color as the control law is switched from the design of Section  to one that handles specifically the high-wind cases. The airplane may or may not get to the desired way point $W_{p2}$, and the results depend on how far from the track the starting position was. However, it is certain that the new design will always move the vehicle to eventually approach the track line regardless of its starting position and orientation.

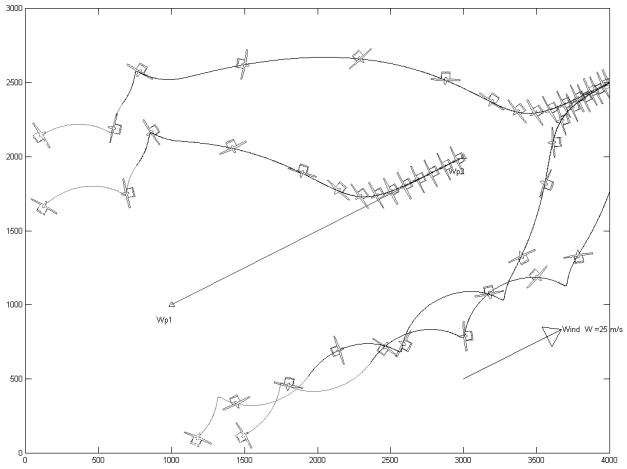


**Fig. 18 Modified Control Law to handle High-Wind Cases**

## Conclusions

In this paper, we present the development of a lateral track control for the Aerosonde UAV that offers improved tracking performance over the design currently implemented in the Operational Phase I Aerosonde. The proposed design handles both the low-wind and high-wind cases in a simple manner, and ensures track stability over a wide set of initial conditions. No direct heading measurement is necessary and the only sensors used for the control law are yaw-rate gyro and GPS. Curvature of the intercept path can be easily adjusted using a single design parameter. Two dynamic models have been developed to evaluate the closed-loop performance of the lateral tracker. The simple kinematic model is found to be useful in the early development of the design parameters. However, a more complex nonlinear 6-DOF airplane model will be necessary to assess the vehicle performance in actual flight. Large roll oscillations found in the simulation using the nonlinear 6-dof model are adequately damped with the use of a roll-off filter introduced to the yaw-rate command loop.

## Acknowledgements

The author acknowledges the support of Jonathan Becker from Aerosonde North America in deciphering the Aerosonde autopilot structure, and for the many questions he patiently answered regarding the Aerosonde Simulator. Special thanks go to Prof. Uy-Loi Ly, from Dept. of Aeronautics and Astronautics at the University of Washington, who directed the research work, reviewed and revised the above manuscript. We also acknowledge the support of the Office of Naval Research who provided the funding for the research work presented in this paper.

## References

[1]Holland, G., McGeer, T., and Youngren, H., "Autonomous Aerosondes for Economical Atmospheric Soundings Anywhere on the Globe," *Bull. Amer. Met. Soc.*, , No. 73, 1992.

[2]McGeer, T., *Flight Control Specifications for the Phase 1 Aerosonde*, The Insitu Group, White Salmon, Washington, 1995.

[3]Ly, U.-L., *A Design Algorithm for Robust Low-Order Controller*, SUDAAR No. 536, Department of Aeronautics and Astronautics, Stanford University, 1982.